

Athermal Silicon-on-insulator ring resonators by overlaying a polymer cladding on narrowed waveguides

Jie Teng^{1,2,3*}, Pieter Dumon¹, Wim Bogaerts¹, Hongbo Zhang^{3,4}, Xigao Jian^{3,4},
Xiuyou Han^{2,3}, Mingshan Zhao^{2,3}, Geert Morthier¹, Roel Baets¹

¹ Photonics Research Group, INTEC-department, Ghent University-IMEC, Ghent, B-9000, Belgium

² School of Physics and Optoelectronic Technology, Dalian University of Technology, Dalian, 116023, China

³ Photonics Research Center, Dalian University of Technology, Dalian, 116023, China

⁴ Department of Polymer Science & Materials, Dalian University of Technology, Dalian, 116012, China

* jteng@intec.ugent.be

Abstract: Athermal silicon ring resonators are experimentally demonstrated by overlaying a polymer cladding on narrowed silicon wires. The ideal width to achieve athermal condition for the TE mode of 220nm-height SOI waveguides is found to be around 350nm. After overlaying a polymer layer, the wavelength temperature dependence of the silicon ring resonator is reduced to less than 5 pm/°C, almost eleven times less than that of normal silicon waveguides. The optical loss of a 350-nm bent waveguide (with a radius of 15µm) is extracted from the ring transmission spectrum. The scattering loss is reduced to an acceptable level of about 50dB/cm after overlaying a polymer cladding.

©2009 Optical Society of America

OCIS codes: (130.3120) Integrated optics devices; (230.7370) Waveguides.

References and links

1. K. Maru and Y. Abe, "Low-loss, flat-passband and athermal arrayed-waveguide grating multi/demultiplexer," *Opt. Express* **15**, 18351-18356 (2007).
2. Y. Kokubun, S. Yoneda, and S. Matsuura, "Temperature-independent optical filter at 1.55 µm wavelength using a silica-based athermal waveguide," *Electron. Lett.* **34**, 367-369 (1998).
3. H. Tanobe, Y. Kondo, Y. Kadota, K. Okamoto, and Y. Yoshikuni, "Temperature insensitive arrayed waveguide gratings on InP substrates," *IEEE Photon. Technol. Lett.* **10**, 235-237 (1998).
4. K. Eun-Seok, K. Woo-Soo, K. Duk-Jun, and B. Byeong-Soo, "Reducing the thermal dependence of silica-based arrayed-waveguide grating using inorganic-organic hybrid materials," *IEEE Photon. Technol. Lett.* **16**, 2625-2627 (2004).
5. J. M. Lee, D. J. Kim, H. Ahn, S. H. Park, and G. Kim, "Temperature dependence of silicon nanophotonic ring resonator with a polymeric overlayer," *J. Lightwave Technol.* **25**, 2236-2243 (2007).
6. J. M. Lee, D. J. Kim, G. H. Kim, O. K. Kwon, K. J. Kim, and G. Kim, "Controlling temperature dependence of silicon waveguide using slot structure," *Opt. Express* **16**, 1645-1652 (2008).
7. W. N. Ye, R. Sun, J. Michel, L. Eldada, D. Pant, and L. C. Kimerling, "Thermo-optical Compensation in High-index-contrast Waveguides," 2008 5th IEEE International Conference on Group IV Photonics, 401-403 (2008).
8. Linjie Zhou, Ken Kashiwagi, Katsunari Okamoto, R. P. Scott, N. K. Fontaine, Dan Ding, V. Akella, and S. J. B. Yoo, "Towards athermal optically-interconnected computing system using slotted silicon microring resonators and RF-photonic comb generation," *Appl. Phys. A* **95**, 1101-1109 (2009).
9. M. Uenuma and T. Moooka, "Temperature-independent silicon waveguide optical filter," *Opt. Lett.* **34**, 599-601 (2009).
10. Y. Kokubun, N. Funato, and M. Takizawa, "Athermal Wave-Guides for Temperature-Independent Lightwave Devices," *IEEE Photon. Technol. Lett.* **5**, 1297-1300 (1993).
11. Y. Kokubun, S. Yoneda, and H. Tanaka, "Temperature-independent narrowband optical filter at 1.31 µm wavelength by an athermal waveguide," *Electron. Lett.* **32**, 1998-2000 (1996).
12. M. W. Pruessner, T. H. Stievater, M. S. Ferraro, and W. S. Rabinovich, "Thermo-optic tuning and switching in SOI waveguide Fabry-Perot microcavities," *Opt. Express* **15**, 7557-7563 (2007).

13. I. Kiyat, A. Aydinli, and N. Dagli, "Low-power thermo-optical tuning of SOI resonator switch," *IEEE Photon. Technol. Lett.* **18**, 364-366 (2006).
 14. H. B. Zhang, J. Y. Wang, L. K. Li, Y. Song, M. S. Zhao, and X. G. Jian, "Synthesis of liquid polysiloxane resins and properties of cured films," *Thin Solid Films* **517**, 857-862 (2008).
 15. W. Bogaerts, R. Baets, P. Dumon, V. Wiaux, S. Beckx, D. Taillaert, B. Luyssaert, J. Van Campenhout, P. Bienstman, and D. Van Thourhout, "Nanophotonic waveguides in silicon-on-insulator fabricated with CMOS technology," *J. Lightwave Technol.* **23**, 401-412 (2005).
 16. W. Bogaerts, D. Taillaert, B. Luyssaert, P. Dumon, J. Van Campenhout, P. Bienstman, D. Van Thourhout, R. Baets, V. Wiaux, and S. Beckx, "Basic structures for photonic integrated circuits in silicon-on-insulator," *Opt. Express* **12**(2004).
 17. D. Taillaert, F. Van Laere, M. Ayre, W. Bogaerts, D. Van Thourhout, P. Bienstman, and R. Baets, "Grating couplers for coupling between optical fibers and nanophotonic waveguides," *Jpn.J.Appl.Phys. Part 1-Regular Papers Brief Communications & Review Papers* **45**, 6071-6077 (2006).
 18. P. Dumon, W. Bogaerts, V. Wiaux, J. Wouters, S. Beckx, J. Van Campenhout, D. Taillaert, B. Luyssaert, P. Bienstman, D. Van Thourhout, and R. Baets, "Low-loss SOI photonic wires and ring resonators fabricated with deep UV lithography," *IEEE Photon. Technol. Lett.* **16**, 1328-1330 (2004).
 19. S. K. Selvaraja, P. Jaenen, S. Beckx, W. Bogaert, P. Dumon, D. Van Thourout, and R. Bates, "Silicon nanophotonic wire structures fabricated by 193nm optical lithography," 2007 IEEE Leos Annual Meeting Conference Proceedings, Vols 1 and 2, 48-49 (2007).
-

1. Introduction

Modern telecommunication and biomedical engineering demand for compact multifunctional photonic circuits with low cost, good performance and high reliability. Silicon photonic integrated circuits with a high index contrast promise to meet this criterion by mature CMOS fabrication technology. The future roadmap is to integrate sensing functions, photonic functions, electronic functions and thermal control elements on one single chip. However, since silicon has a quite large thermo-optic coefficient ($dn/dT=1.8 \times 10^{-4}/^{\circ}\text{C}$), external heaters or coolers have to be employed to stabilize the chip temperature. This element takes extra space and consumes extra power.

There are a number of ways to achieve athermal devices by designing specific waveguides circuits [1-3]. Among those methods, the simplest and applicable to most devices (e.g. ring resonator, Mach-Zehnder interferometer, Arrayed Waveguides Grating etc.) is to overlay a polymer cladding on the circuit and use the polymer's negative thermo-optic (TO) coefficient to counterbalance the waveguide core's positive TO coefficient. Temperature independent silica based Add-Drop filters and AWGs have been successfully demonstrated by overlaying a polymer cladding in the past few years [2, 4]. The biggest obstacle in using this method for silicon waveguides is that silicon has a quite large thermo-optic coefficient, of the same order of magnitude as for the polymer material ($10^{-4}/^{\circ}\text{C}$) and almost twenty times larger than that of silica. This requires almost half of the light to penetrate out of the silicon core into the polymer cladding to achieve the athermal condition.

Recently, some groups experimentally demonstrated the possibility of achieving athermal silicon waveguides by using this method [5-9]. In order to have more light into the polymer cladding, the dimension of the silicon waveguides is highly reduced either by narrowing the core width [5, 9] or by thinning the core height [7], or by using a slot waveguide structure [6, 8]. Narrowed waveguides and slot waveguides impose big challenges for fabrication. E-beam writing is employed in [5, 6, 8] and results in large losses. Inaccurate control of the narrowed waveguide width or slot width seems unsatisfactory for athermal condition of silicon waveguides. E-beam writing itself is also less efficient for mass fabrication.

In this paper, we successfully achieve athermal silicon ring resonators by overlaying a polymer PSQ-LH cladding on uniform narrowed silicon waveguides. The ideal width for athermal silicon waveguides (with a height of 220nm) is found to be around 350nm. The wavelength temperature shift of the silicon ring resonator is reduced to less than 5 pm/ $^{\circ}\text{C}$. The athermal ring resonators have lower loss than other proposed athermal rings.

2. Theoretical analysis

In 1993, Y. Kokubun et al first proposed to achieve the athermal waveguides by overlaying a polymer cladding on silica waveguides [10]. Later an athermal optical filter was successfully achieved by this method [2, 11]. The principle of that technique is quite simple: to use the polymer's negative TO coefficient to compensate silica's positive TO coefficient. This method is applicable to most passive devices; e.g. Fabry-Perot resonators, DBR filters, Mach-Zehnder interferometers and arrayed waveguides gratings (AWG).

Taking the ring resonator as an example, the temperature dependence of the resonance wavelength can be expressed as follows [2, 11],

$$\frac{d\lambda_m}{dT} = \left(\frac{1}{L} \cdot \frac{dS}{dT} \right) \frac{\lambda_m}{n_{eff}} = \left(n_{eff} \cdot \alpha_{sub} + \frac{dn_{eff}}{dT} \right) \frac{\lambda_m}{n_g} \quad (1)$$

where λ_m is the resonant wavelength; n_{eff} is effective index of the waveguide; S is the optical length defined as $S = n_{eff} \cdot L$; α_{sub} is the substrate expansion coefficient; n_g is the group index of the waveguide. For silicon optical waveguides, the dispersion effect has to be considered when calculating the shift of the resonance wavelength.

The athermal condition is achieved when Eq. (1) equals to zero. Normally silicon is used as substrate and the thermal expansion coefficient of Si is on the order of 10^{-6} [2, 11] ($\alpha_{sub} = 2.6 \times 10^{-6}/^\circ\text{C}$); dn_{eff}/dT depends on the thermo-optic coefficient of the core material and cladding material. For highly confined waveguide, dn_{eff}/dT is of the same order as the TO coefficient of the core material: $TO_{silica} = 1 \times 10^{-5}/^\circ\text{C}$ [2, 11]; $TO_{silicon} = 1.8 \times 10^{-4}/^\circ\text{C}$ [12, 13]. As the TO coefficient of polymer material is of the order of $-(1\sim 3) \times 10^{-4}/^\circ\text{C}$, athermal silica waveguides can be easily achieved with only a little fraction of light penetrating out of the core while athermal silicon waveguides require almost half of the light out of the core.

To obtain athermal silicon waveguides, the dimension of the silicon waveguide should be highly reduced to allow more light coming out of the core waveguides. In this paper, a standard SOI (silicon on insulator) structure with a height of 220nm is used for designing the athermal waveguides (Fig. 1). Polymer PSQ-LH with a large TO coefficient of $-2.4 \times 10^{-4}/^\circ\text{C}$ and low loss at 1550nm is chosen as the cladding material [14]. By using Eq.(1), $d\lambda_m/dT$ of the TE mode for different widths of the SOI waveguide is calculated (Fig.2) by FIMMWAVE (©PhotonDesign Ltd). The value of dn_{eff}/dT of SOI straight waveguide is used for calculation instead of that of bent SOI waveguide. The calculation show that there's almost no difference between both values of dn_{eff}/dT . The index and TO coefficient of silicon is set as 3.4757 (20°C) and $1.8 \times 10^{-4}/^\circ\text{C}$ [12, 13]. The index of silica and polymer PSQ-LH is set as 1.444 (20°C) and 1.515 (20°C). As shown in Fig.2, the $d\lambda_m/dT$ of standard 500nm width SOI waveguides with a polymer-clad is near to $+60\text{pm}/^\circ\text{C}$; by narrowing the width of SOI waveguides, $d\lambda_m/dT$ is reduced to zero and then becomes negative. From the theoretical calculation results, the ideal width for athermal silicon waveguide is around 306nm (Fig.2).

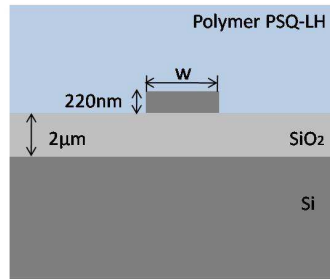


Fig. 1. SOI waveguide cross-section structure

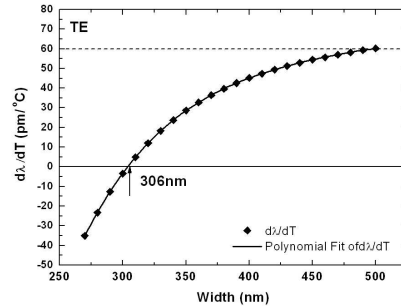


Fig. 2. Calculated wavelength temperature dependence of TE mode for SOI waveguides with a polymer overlay as a function of waveguide widths

3. Fabrication and measurement results

3.1 Waveguides fabrication

As shown in Fig. 2, athermal SOI waveguides are achieved when a relatively small waveguide core width is used. And the temperature dependence of the resonance wavelength (for ring resonators) becomes more sensitive to the waveguide core width as the core width decreases. Therefore, high quality, high resolution fabrication technologies are required for these narrow silicon waveguides. The narrow SOI waveguides in this paper are fabricated by deep UV lithography with standard CMOS fabrication technology [15, 16]. This technology offers both the required resolution and the throughput for commercial application.

The SOI wafer with a silicon thickness of 220nm and a oxide layer of 2 μ m is used for this work (Fig. 1). Simple racetrack ring resonators with different waveguide widths are designed and fabricated. Referring to the theoretical calculation results mentioned above, the ideal width for the athermal waveguides is around 306nm. So ring resonators with a narrow width of 300nm and 350nm are designed on the mask. The waveguide width can be adjusted a little by varying the exposure dose when doing deep UV lithography[15, 16]. The SEM pictures of the fabricated ring resonators are shown in Fig. 3. The racetrack ring resonators are designed with different radius, a coupling length of 2 μ m, and a gap of 180nm.

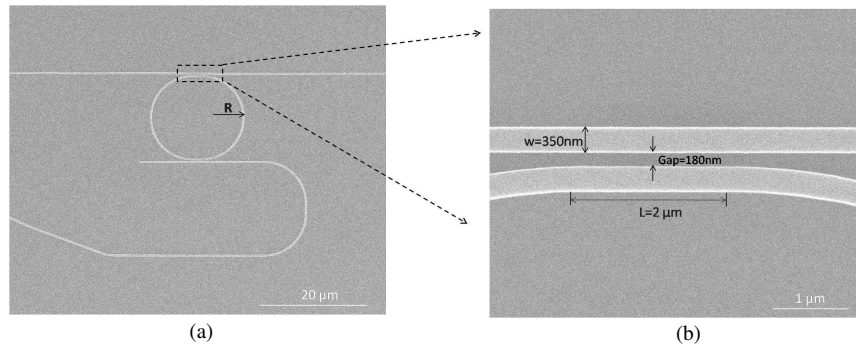


Fig. 3. SEM pictures of fabricated ring resonators with a width of 350nm (a) the whole ring (b) the coupling region

3.2 Measurement results

To couple light in and out of the silicon wires from a single mode fiber, shallow etched (70nm) gratings are fabricated near the edge of each waveguides[15-17]. This kind of grating has polarization selectivity and therefore the transmission spectrum measured below are all for TE mode polarization. A broadband infrared light source SLED (super-luminescent light-emitting diode) and spectrum analyzer (Agilent 86140B) are used for the characterization of the transmission spectrum of the ring resonator. To measure the transmission spectrum at different temperatures, the sample is mounted on a heating system to accurately control the chip temperature. Fig.4 shows the measured transmission spectrum of a ring resonator (Width=350nm, Gap=180nm, L=2 μ m, R=15 μ m) for temperatures from 10°C to 50°C with an interval of 10°C. By linear fitting of one resonance wavelength at different temperatures, the wavelength temperature dependence $d\lambda/dT$ is extracted (Fig.4(b)(d)). As shown in Fig.4, the wavelength temperature dependence of the 350nm-width ring resonator is reduced from 54.2pm/°C to -4.9pm/°C after overlaying a polymer PSQ-LH cladding. The ideal width for the athermal ring resonator is found to be around 350nm, a little different from the theoretically calculated value of 306nm.

It has to be pointed out that the value $d\lambda/dT$, which is calculated from the linear fitting of the data, is not an absolute value. The spectrum analyzer resolution, temperature measurement range, the numbers of the data taking into account for linear fitting all have some influence on the value of $d\lambda/dT$, especially when the waveguide width is near the athermal condition and the $d\lambda/dT$ slope is quite small. Measurements have been done repeatedly and the results are reproducible. A conclusion can be drawn that the wavelength temperature dependence of silicon ring resonator can be reduced to less than 5 pm/°C after deposition of a polymer cladding, almost eleven times less than that of normal silicon waveguides.

3.3 Loss estimation

Reducing the silicon waveguide width imposes a big challenge on fabrication technology. The extent to which the waveguide width can be reduced is compromised by the scattering loss caused by fabrication technology. The loss of the silicon wires increases exponentially when the waveguide width decreases [15, 16, 18]: from 2.4dB/cm for a 500nm-wire, over 7.4dB/cm for a 450nm-wire, to 34dB/cm for a 400nm-wire. Recently, the loss rate of 450nm-silicon waveguides has been reduced down to be about 3dB/cm [19].

The optical loss of the 350nm-ring waveguide is estimated by fitting the transmission spectrum of the ring resonator. Figure 5 shows the transmission spectrum of the ring resonator (Width=350nm, Gap=180nm, L=2 μ m, R=15 μ m) at room temperature before and after overlaying a polymer cladding.

By fitting of the spectrum with a Lorenz-function in Fig. 5, the total loss of the bending waveguides and the coupling coefficient are extracted. An interesting phenomenon is found.

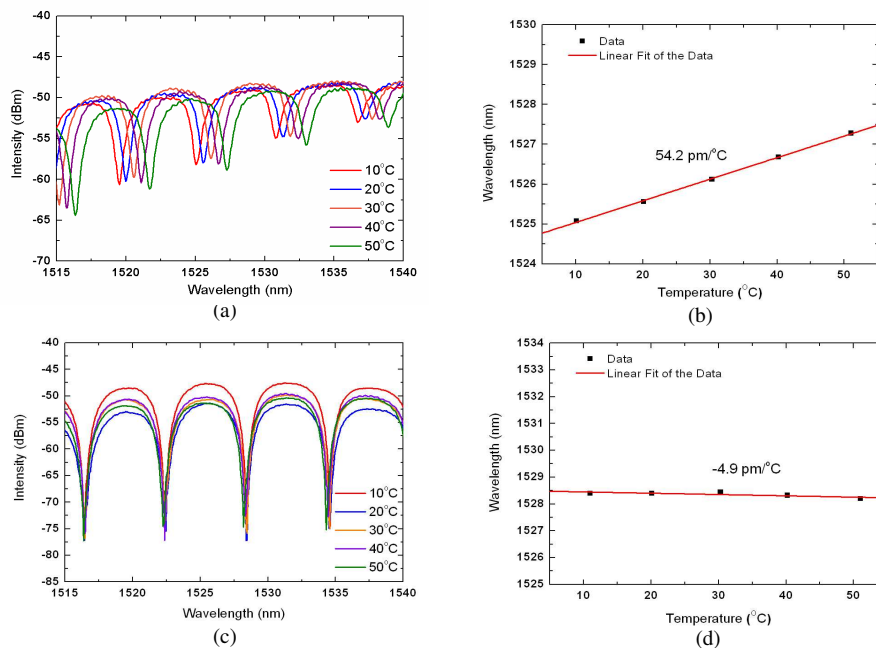


Fig. 4. (a) Transmission spectrum of a ring resonator with width of 350nm at different temperatures before overlaying a polymer cladding (b) Linear fit of the wavelength versus temperatures (c) Transmission spectrum of a ring resonator with width of 350nm at different temperatures after overlaying a polymer cladding (d) Linear fit of the wavelengths versus temperatures (Width=350nm, Gap=180nm, L=2 μ m, R=15 μ m)

For the width of 350nm and a ring radius of 15 μ m, the fitted total loss of the bending waveguide is about 300dB/cm before overlaying a polymer cladding. After overlaying a polymer cladding, the fitted total loss is reduced to about 50dB/cm, which is the same order as for a 450nm width and a 5 μ m ring radius [18]. The reduced loss of the bending waveguides is due to a reduction of the scattering loss for a decrease of the index contrast between the core and the cladding after overlaying a polymer cladding.

The coupling coefficient (the power percentage coupled to the ring) between the ring and the straight waveguides is increased from 50% to 75% after a polymer cladding (Fig. 5). Since our aim is to test thermal behavior of the ring resonator, the coupling between the ring and the straight waveguide has not been optimized. The Q factor of the ring should decrease

as the coupling power increases. Contrarily, the Q factor has significantly increased after overlaying a polymer cladding (Fig. 5), which also indicates a loss reduction after overlaying a polymer cladding.

In addition, the athermalization method proposed here is also applicable to multipath interferometric devices, like MZ interferometers and AWG. Simple athermal MZ interferometers with a waveguide width of 350nm have also been achieved by this method.

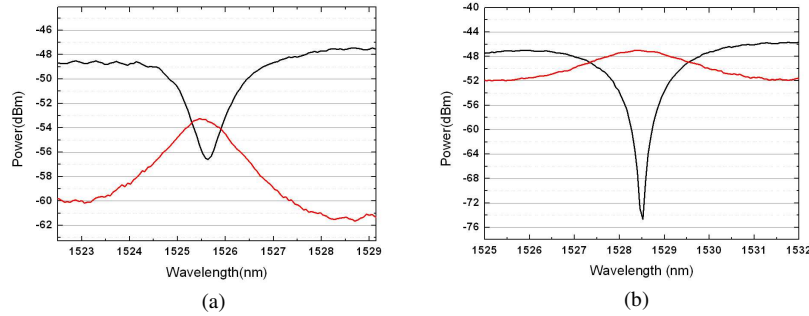


Fig. 5. Transmission spectrum of ring resonator with width of 350nm at room temperature (a) Before overlaying a polymer cladding (b) After overlaying a polymer cladding (With a black line for the Through port and red line for the Drop port, Ring resonator parameters: Width=350nm, Gap=180nm, L=2 μ m, R=15 μ m)

4. Conclusion

Athermal silicon ring resonators are experimentally demonstrated in this paper. Standard deep UV lithography and dry etching are used for fabricating such silicon wires. By overlaying a polymer layer on narrowed silicon wires, the wavelength temperature dependence of a silicon ring resonator is reduced to less than 5 pm/ $^{\circ}$ C, almost eleven times less than air-clad silicon waveguides. The ideal width to achieve athermal condition for the TE mode of 220nm-height SOI waveguides is found to be around 350nm.

Acknowledgements

The fabrication of the SOI circuits was done by CEA-LETI through ePIXfab (www.epixfab.eu). Jie Teng acknowledges CSC scholarship and Ghent University BOF Co-funding for financial support. This work is also partly supported by NSFC No.60577014.